Chemical Science

ROYAL SOCIETY OF CHEMISTRY

EDGE ARTICLE

View Article Online
View Journal | View Issue

Cite this: *Chem. Sci.*, 2025, **16**, 13684

All publication charges for this article have been paid for by the Royal Society of Chemistry

Received 17th February 2025
Accepted 6th June 2025

DOI: 10.1039/d5sc01244a

rsc.li/chemical-science

Ensembles of cationic conjugated polymer and anionic platinum(II) complexes: from FRET properties to application studies in *E. coli* imaging and singlet oxygen generation†

Angela Lok-Yin So,‡[a] Jungu Guo,‡[a] Huanxiang Yuan,[b] Qi Shen,[b] Eric Ka-Ho Wong,[a] Shu Wang *[b] and Vivian Wing-Wah Yam *[a]

A series of anionic alkynylplatinum(II) complexes with terpyridine (tpy) or 2,6-bis(benzimidazol-2′-yl) pyridine (bzimpy) as the tridentate *N*-donor pincer ligand has been synthesized and characterized. These complexes are found to form ensembles with a cationic poly(fluorene-*co*-phenylene) derivative (PFP-NMe_3^+) through electrostatic, Pt(II)···Pt(II) and π–π stacking interactions. Förster resonance energy transfer (FRET) has been found to take place, consequently gave rise to fluorescence quenching of the polymer donor and the emergence of low-energy emission from the platinum(II) complex assemblies. The spectroscopic and FRET properties of the two-component systems have been investigated by UV-vis absorption, emission and Stern–Volmer quenching studies. Pathogen imaging and photodynamic therapy (PDT) studies using the polymer–platinum(II) complex ensembles have demonstrated better performance compared to that using PFP-NMe_3^+ only, which highlights the potential of this class of ensembles for various biological applications.

Introduction

Platinum(II) complexes with a d^8 electronic configuration and square-planar geometry have attracted much attention due to their notable propensity to undergo supramolecular self-assembly and form higher-ordered structures.[1–18] In particular, platinum(II) polypyridine complexes represent one of the most extensively studied classes of complexes,[17–23] as the extent of non-covalent interactions including metal–metal and π–π stacking interactions between the complexes has been reported to be sensitive to subtle changes in microenvironments including pH,[21,23] temperature,[24,25] counter anion,[26] solvent composition,[14,22] and the presence of polyelectrolytes.[27] These interactions contribute to their interesting spectroscopic, luminescence and morphological properties. The rich and diverse properties of platinum(II) polypyridine complexes associated with Pt(II)···Pt(II) and π–π stacking interactions can further be manipulated by rational molecular design that facilitates specific interactions between the complexes and molecules of interest, which endow this class of complexes with potential applications in the fields of biology and materials science.[28–32]

In addition to investigation into the self-assembly of single-component systems comprising only platinum(II) complexes, research effort has been made to develop multi-component supramolecular systems with enhanced complexity and intriguing properties that are not exhibited by the individual components.[33–36] Polyelectrolytes, a class of highly water-soluble macromolecules comprising a large number of ionic pendants, have played an important role in the recent development of new functional materials and biomedical applications.[37–40] With further structural functionalization by the introduction of an extensive π-conjugated polymer backbone, conjugated polyelectrolytes (CPEs) could be obtained. Compared to non-conjugated polyelectrolytes, CPEs are electronically connected by a π-conjugated molecular wire backbone, allowing amplified fluorescence quenching to take place through efficient energy transduction in the presence of fluorescence quenchers.[41–43] With unique optical and electronic properties, CPEs have been found to not only induce self-assembly of an oppositely charged platinum(II) complex through electrostatic, Pt(II)···Pt(II) and π–π stacking interactions,[35] but also act as fluorophore donors which can facilitate Förster resonance energy transfer (FRET) to platinum(II) acceptors upon the formation of polymer–metal complex ensembles. It has been shown that the spectroscopic

[a]*Institute of Molecular Functional Materials and Department of Chemistry, The University of Hong Kong, Pokfulam Road, Hong Kong, PR China. E-mail: wwyam@hku.hk*

[b]*Beijing National Laboratory for Molecular Sciences, Key Laboratory of Organic Solids, Institute of Chemistry, Chinese Academy of Sciences, Beijing, PR China. E-mail: wangshu@iccas.ac.cn*

† Electronic supplementary information (ESI) available. See DOI: https://doi.org/10.1039/d5sc01244a

‡ These authors contributed equally to this work.

properties of the two-component system are governed by multiple factors including the FRET efficiency of the donor–acceptor pair, excited-state chemistry of both the CPEs and the platinum(II) complexes, as well as interactions of other biomolecules with the ensemble.[33–36] In particular, studies have demonstrated that two-component CPE–platinum(II) complex ensembles containing charged poly(phenylene ethynylene) (PPE) and poly(fluorene-*co*-phenylene) (PFP) have achieved selective and sensitive detection of pH as well as various biological substances including human serum albumin (HSA) and G-quadruplex deoxyribonucleic acid (DNA).[33,34,44] Such a unique and drastic spectroscopic response of the FRET ensembles associated with long-lived triplet metal–metal-to-ligand charge transfer (^{3}MMLCT) emission in the near-infrared (NIR) region originating from the aggregate form of platinum(II) complexes renders them competitive candidates for applications in biological sensing and imaging.[28,45–48]

Despite a number of reports on the supramolecular ensembles of anionic polyelectrolytes and cationic platinum(II) polypyridine complexes aimed at improving the understanding of interactions between CPEs and platinum(II) complexes,[27,33–36,49] studies on interactions between cationic CPEs and anionic platinum(II) polypyridine complexes remain relatively scarce, not to mention the relevant ensemble systems and their potential applications in the biological field.[27,32,33,35] In view of the emerging significance of the cationic poly(fluorene-*co*-phenylene) derivative (PFP-NMe$_3^+$) for its applications in biological imaging and photodynamic therapy (PDT),[50–56] we herein present the studies on ensembles between PFP-NMe$_3^+$ and a series of anionic platinum(II) complexes **1–3** with terpyridine (tpy) or 2,6-bis(benzimidazol-2′-yl)pyridine (bzimpy) tridentate *N*-donor pincer ligands (Scheme 1). A control cationic complex **4** has also been synthesized to investigate the role of charge in the formation of polymer–complex ensembles. The photophysical properties of the supramolecular systems as a result of FRET from PFP-NMe$_3^+$ to the aggregate species of the complexes have been examined. Further applications of the ensembles as a biological imaging tool and a PDT photosensitizer towards pathogens have been investigated. It is envisaged that the current study would pave the way for potential biological applications of the two-component systems by taking advantage of the unique luminescence and supramolecular properties of the ensembles.

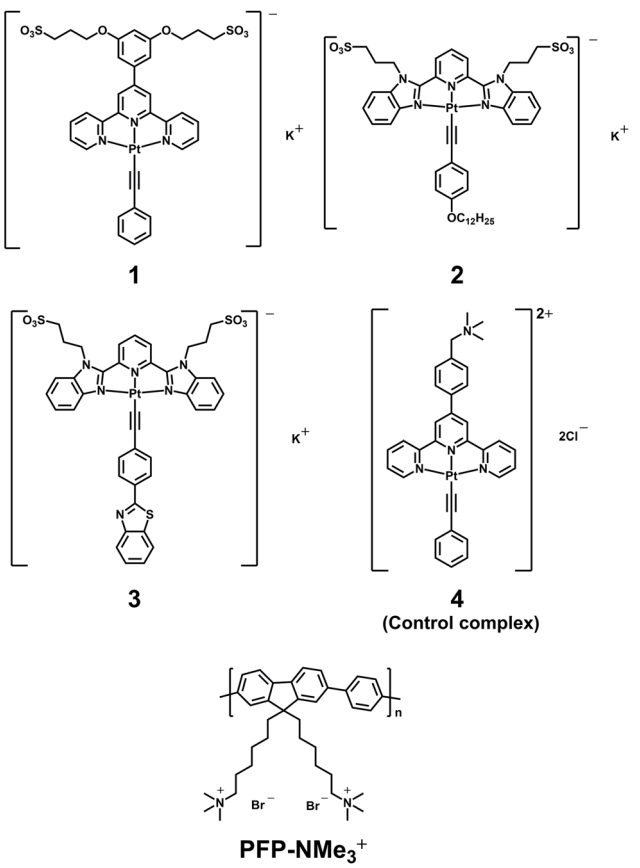

Scheme 1 Molecular structures of platinum(II) complexes **1–4** and conjugated polyelectrolyte PFP-NMe$_3^+$.

Results and discussion

Complexes **1–4** were obtained by dehydrohalogenation reactions of chloroplatinum(II) precursor complexes with the corresponding alkynes in degassed solutions in the presence of a catalytic amount of copper(I) iodide and amine under an inert atmosphere.[22,46] The complexes were subjected to purification by recrystallization, followed by salt metathesis reaction to afford the complexes of desired counter-ions. All of the platinum(II) complexes were characterized by ^{1}H nuclear magnetic resonance (NMR), ^{13}C{^{1}H} NMR spectroscopy and high-resolution electrospray ionization mass spectrometry (HR-ESI-MS). Details of the synthesis and characterization data are presented in the ESI.†

The photophysical properties of the conjugated polymer and complexes have been investigated by UV-vis absorption studies. The electronic absorption spectrum of PFP-NMe$_3^+$ in water displays an absorption band centered at 375 nm, which is assigned to the $\pi \rightarrow \pi^*$ transition of the conjugated polymer (Fig. S1a†).[44] For the platinum(II) complexes, intense absorption bands at 288–334 nm and less intense absorption bands at 440–450 nm are observed in the absorption spectra of **1** and **4** recorded in aqueous solution (Fig. S1b†). The high-energy absorption bands are tentatively assigned to spin-allowed intraligand (IL) [$\pi \rightarrow \pi^*$] transitions of the terpyridine and alkynyl ligands, while the low-energy absorption bands are assigned to an admixture of metal-to-ligand charge transfer (MLCT) [dπ(Pt) $\rightarrow \pi^*$(tpy)] and ligand-to-ligand charge transfer (LLCT) [π(alkynyl) $\rightarrow \pi^*$(tpy)] transitions.[33] Absorption profiles of **2** and **3** in a solvent mixture of water–DMSO (19 : 1, v/v) are found to be similar to those of **1** and **4** in water, with the high-energy and low-energy absorptions being ascribed to IL [$\pi \rightarrow \pi^*$] transitions of the bzimpy and alkynyl ligands, and an admixture of MLCT [dπ(Pt) $\rightarrow \pi^*$(bzimpy)] and LLCT [π(alkynyl) $\rightarrow \pi^*$(bzimpy)] transitions respectively. The UV-vis absorption data of PFP-NMe$_3^+$ and complexes **1–4** have been summarized in Table S1.†

The supramolecular assembly behaviors between PFP-NMe_3^+ and platinum(II) complexes in aqueous solution have been investigated by UV-vis absorption studies. Upon addition of **1** to an aqueous solution of PFP-NMe_3^+, a decrease in the high-energy absorption band at 375 nm and a pronounced growth of a low-energy absorption band at 430–600 nm are observed with a well-defined isosbestic point at 355 nm (Fig. 1a). The corresponding studies have also been performed in water–DMSO (19 : 1, v/v) mixture for **2** and **3**, in which an increase in absorption bands at 280–380 nm and a notable growth of the low-energy absorption band at 430–600 nm are observed (Fig. 1b and c). While the rise of the low-energy absorption bands can be partly rationalized by the increase in the absorbance at 450–480 nm due to increasing amounts of **1–3**, the red shift of the band maxima as well as a concomitant rise of lower-energy absorption tails at 500–600 nm observed cannot be explained by the increase in concentration of the complexes. It is worth noting that the increase in the low-energy absorption band is more significant than that of the addition spectrum of PFP-NMe_3^+ and the platinum(II) complex (Fig. S2†), suggestive of a more extensive assembly in the two-component system. Such absorption tails are thus assigned to MMLCT transitions, resulting from the electrostatic interactions of the platinum(II) complexes with the oppositely charged PFP-NMe_3^+, which leads to the formation of new aggregate species of platinum(II) complexes *via* Pt(II)···Pt(II) and π–π stacking interactions upon their electrostatic co-assembly with the oppositely charged PFP-NMe_3^+.

To gain more insight into the interaction between PFP-NMe_3^+ and the platinum(II) complexes, the emission spectra of PFP-NMe_3^+ in aqueous medium with various concentrations of complexes **1–3** upon photoexcitation at $\lambda = 355$ nm have been systematically investigated. Gradual drops in the intensity of emission bands at 415–422 nm are observed upon increasing the concentration of complexes from 0 to 50 μM, which are accompanied by the emergence of lower-energy emissions centered at 700–778 nm (Fig. 2, S3 and S4†). This, along with the absorption changes, contributes to an obvious change in color from colorless to yellow and a shift in the emission color of the solution from blue to red, both of which are visible to the naked eye (Fig. 3). Upon cooling the solution of the ensemble of PFP-NMe_3^+ and **3** from 363 to 303 K, a luminescence enhancement along with a red shift of the low-energy emission band from 660 to 670 nm is observed (Fig. S5†). While the less favorable non-radiative decay at lower temperatures can partially explain the increase in emission intensity, the red shift of the emission band is associated with the presence of more extensive Pt(II)···Pt(II) and π–π stacking interactions in the two-component ensemble. Thus, the lower-energy emission band is assigned to originate from a ^{3}MMLCT excited state. A linear relationship between the ^{3}MMLCT emission intensity and the concentration of **1** is found upon addition of **1** to a solution of PFP-NMe_3^+ (Fig. S3d†), which does not resemble the cases of **2** and **3**. A further comparison study shows that the enhancement of the low-energy emission in the presence of the CPE is more significant than that observed from increasing the concentration of **1** over the same concentration range in the absence of the CPE (Fig. S6†), hence demonstrating the polymer-induced aggregation behavior of **1**. Together with the results of the UV-vis absorption studies, the emissions in the NIR region are ascribed to be of ^{3}MMLCT origin. Moreover, a red-shifted ^{3}MMLCT emission maximum of **1** compared to those of **2** and **3** with the bzimpy pincer ligand has also been observed in the emission spectra,

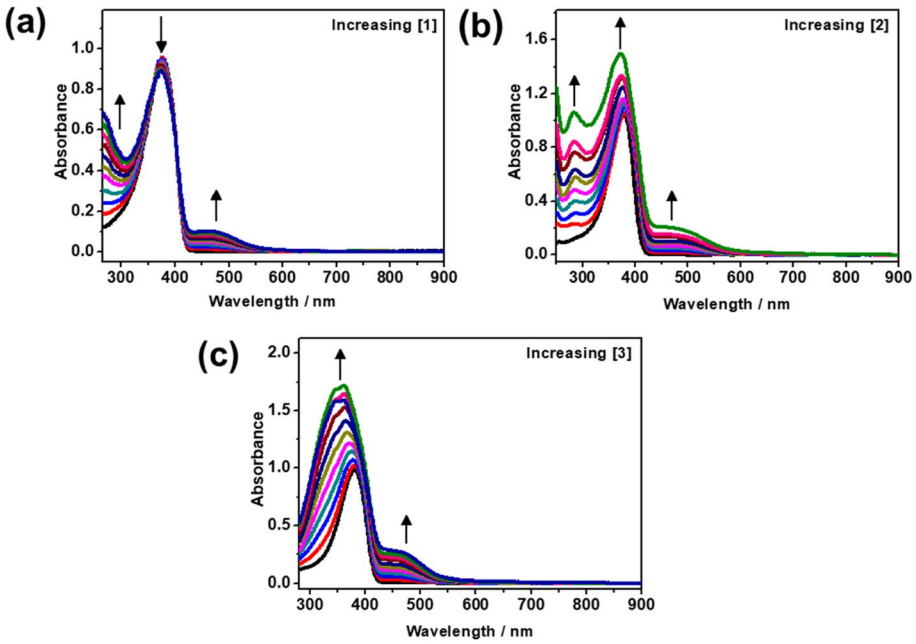

Fig. 1 Electronic absorption spectral changes of PFP-NMe_3^+ (50 μM) upon addition of different concentrations of (a) **1** in water as well as (b) **2** and (c) **3** in water–DMSO (19 : 1, v/v) mixture (0–50 μM).

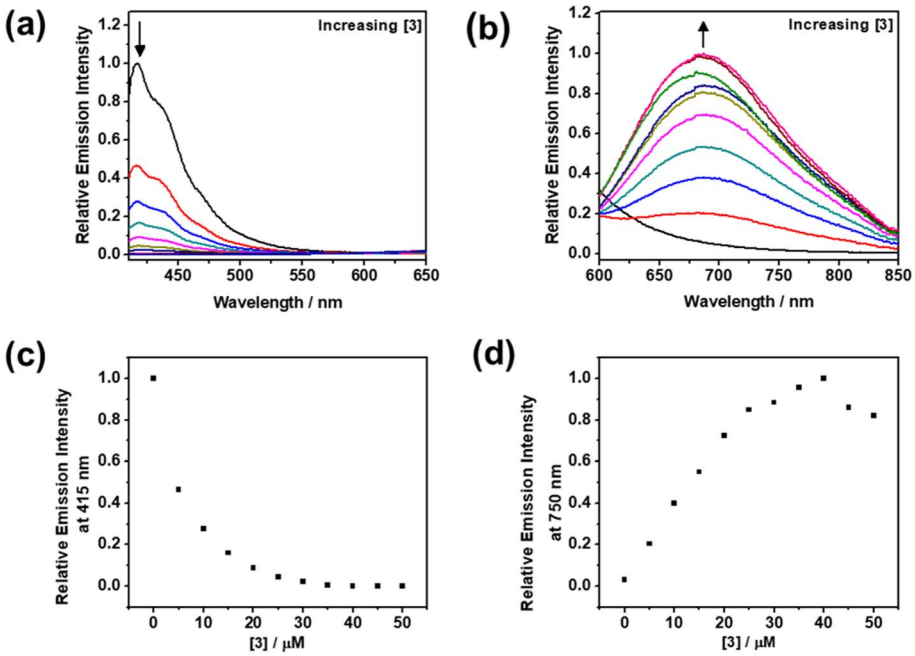

Fig. 2 Emission spectral changes of PFP-NMe_3^+ (50 μM) in water–DMSO (19 : 1, v/v) mixture upon addition of different concentrations of **3** (0–50 μM) in the range of (a) 400–650 nm and (b) 600–850 nm. (c) A plot of relative emission intensity at 415 nm against [**3**]. (d) A plot of relative emission intensity at 750 nm against [**3**]. An excitation wavelength of 385 nm was used.

which is in agreement with previous studies on alkynylplatinum(II) terpyridine and bzimpy complexes.[44,57]

In light of their potential FRET properties, evidenced by the decrease in higher-energy emissions originating from the $^1[\pi \rightarrow \pi^*]$ excited states of PFP-NMe_3^+ indicating quenching events, and the emergence of low-energy emission bands brought about by increasing concentrations of complexes **1–3**, the intermolecular deactivation processes between the conjugated polymer and the platinum complexes have been further examined by Stern–Volmer (SV) experiments. Apart from static quenching that occurs at lower concentrations of the platinum(II) complexes,[58] a more efficient quenching of PFP-NMe_3^+

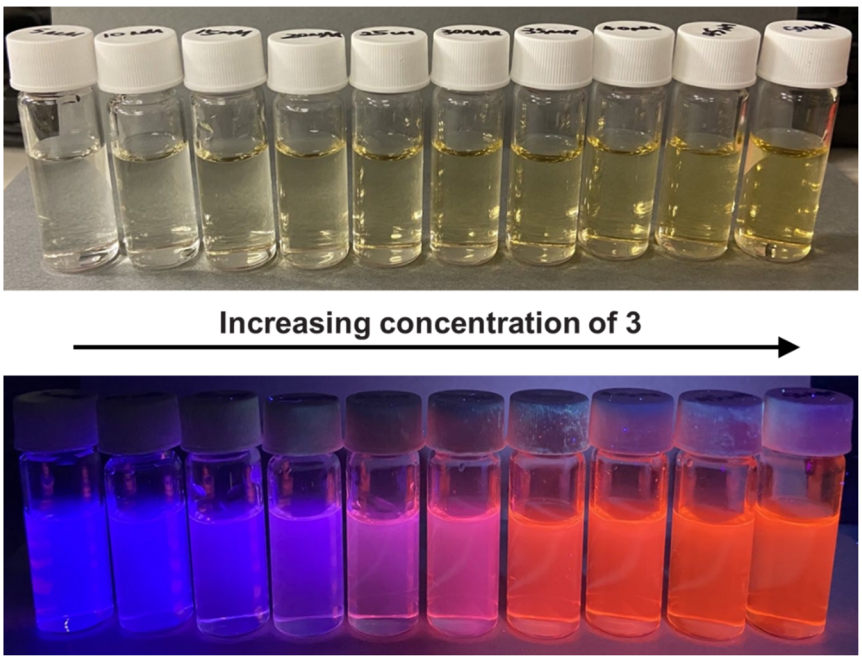

Fig. 3 Photographs showing a series of solutions comprising PFP-NMe_3^+ (50 μM) and different concentrations of **3** (0–50 μM) in water–DMSO (19 : 1, v/v) mixture under natural light (top) and UV irradiation (bottom).

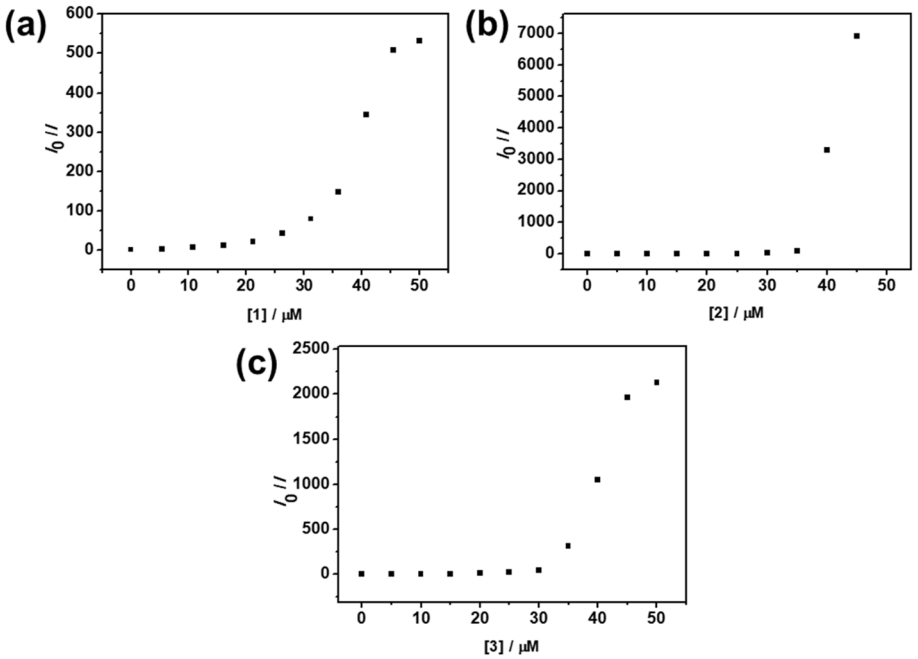

Fig. 4 SV plot for the emission quenching of PFP-NMe_3^+ (50 μM) by different concentrations of (a) **1** (0–50 μM) in water as well as (b) **2** and (c) **3** in water–DMSO (19 : 1, v/v) mixture. The emission intensities are monitored at 422 nm (**1**) and 415 nm (**2** and **3**) with increasing concentration of platinum(II) complexes. Excitation wavelengths of 355 nm for **1** as well as 385 nm for **2** and **3** were used.

is found when the concentrations of complexes reach 35–40 μM, as supported by the upward curvature of the SV plots and the increased Stern–Volmer quenching constants (K_{SV}) (Fig. 4 and Tables S2–S4†). The more efficient quenching of fluorescence from the conjugated polyelectrolyte can be rationalized by the formation of polymer–metal complex ensembles driven by electrostatic, Pt(II)···Pt(II) and π–π stacking interactions, which could possibly lead to FRET from PFP-NMe_3^+ to the aggregate species of platinum(II) complexes. A control experiment by increasing the concentration of a positively charged complex **4** in an aqueous solution of PFP-NMe_3^+ has been carried out, in which a less efficient fluorescence quenching at 422 nm is observed (Fig. S7†). This confirms the important role of the anionic nature of **1–3** endowed by the negatively charged sulfonate pendant groups in facilitating the electrostatic interactions between the polyelectrolyte and platinum(II) complexes, with the ensembles further stabilized by Pt(II)···Pt(II) and π–π stacking interactions. Supramolecular assembly between the polyelectrolyte and the complexes gives rise to more efficient intra- and inter-chain diffusions of excitons from PFP-NMe_3^+ to **1–3**, as well as larger spectral overlaps between the low-energy MMLCT absorption band of **1–3** and the emission band of PFP-NMe_3^+ (Fig. S2 and S8†), consequently promoting an efficient FRET with reasonable values of donor–acceptor spectral overlap integral (J) in the order of 10^{15} cm^2 nm^4 mol^{-1} and Förster radius (R_0) of around 59 Å (Table S5†). Electrostatically induced self-assembly of platinum(II) complexes and the related FRET process thereby give rise to a decrease of $^1[\pi \rightarrow \pi^*]$ emission of PFP-NMe_3^+ as well as the enhancement of ^{3}MMLCT emission in the low-energy NIR region, which is in accordance with the results of the UV-vis absorption studies.

To investigate the effect of pH on the formation of the two-component assemblies, the emission spectra of PFP-NMe_3^+ alone, and PFP-NMe_3^+ with the addition of 50 μM of **3** in Tris-HCl buffer (pH 6.0–9.0) have been obtained (Fig. S9†). Similar emission profiles of PFP-NMe_3^+ with slight differences in emission intensities are found in the tested pH range, while effective fluorescence quenching and the emergence of the ^{3}MMLCT emission are observed upon introduction of the platinum(II) complex, suggesting a limited influence of pH on the formation of the FRET ensemble by electrostatic interactions. This can be rationalized by a lack of ability of the quaternary ammonium group to be protonated or deprotonated, and a low pK_a value of the sulfonic acid group of around −1.68.[59] The quaternary ammonium side chains on PFP-NMe_3^+ and the sulfonate pendants on platinum(II) complexes thus remain in their charged states in a wide range of pH and are not sensitive to pH changes. The FRET system hence demonstrates tolerance towards slightly acidic and basic environments.

Due to the highly lipophilic and cationic nature of PFP-NMe_3^+ that enables strong interactions with the negatively charged microbial surface, there have been studies on PFP-NMe_3^+ and their relevant FRET systems as a novel tool to visualize or discriminate pathogens of distinct types.[54,60,61] In light of this, this work has been extended to investigate the behavior of the PFP-NMe_3^+ and platinum(II) complex ensemble in the presence of pathogens by imaging experiments. Confocal images of the selected pathogen *E. coli* reveal strong signals in the blue luminescence channel (425–525 nm) upon incubation with PFP-NMe_3^+ at 37 °C for 30 minutes, indicating the binding of the amphiphilic conjugated polyelectrolyte to the negatively charged bacterial surface (Fig. 5a–d). Upon incubation with the

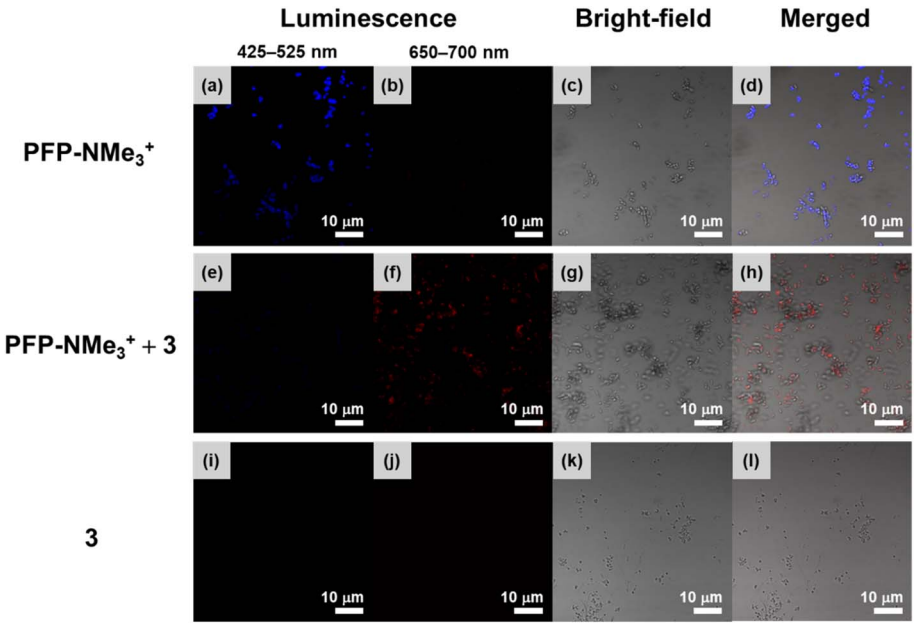

Fig. 5 Confocal images of *E. coli* incubated with (a–d) PFP-NMe_3^+ (50 μM), (e–h) ensemble of PFP-NMe_3^+ and **3** (50 μM each) as well as (i–l) **3** (50 μM) at 37 °C for 30 minutes. (a, e and i) Luminescence collected at 425–525 nm; (b, f and j) luminescence collected at 650–700 nm; (c, g and k) bright-field; and (d, h and l) merged confocal images are shown in the corresponding figures. An excitation wavelength of 405 nm was used.

ensemble of PFP-NMe_3^+ and **3**, the binding ability towards *E. coli* is found to be retained as revealed from the confocal images. Interestingly, the disappearance of signals in the blue luminescence channel, accompanied by the emergence of emission in the red luminescence channel (650–700 nm), is observed (Fig. 5e–h). In agreement with the results from emission studies, this is attributed to the formation of the polymer–metal complex aggregate resulting in an efficient FRET, which gives rise to the growth of the low-energy ^{3}MMLCT emission of **3** accompanied by quenching of the high-energy fluorescence of

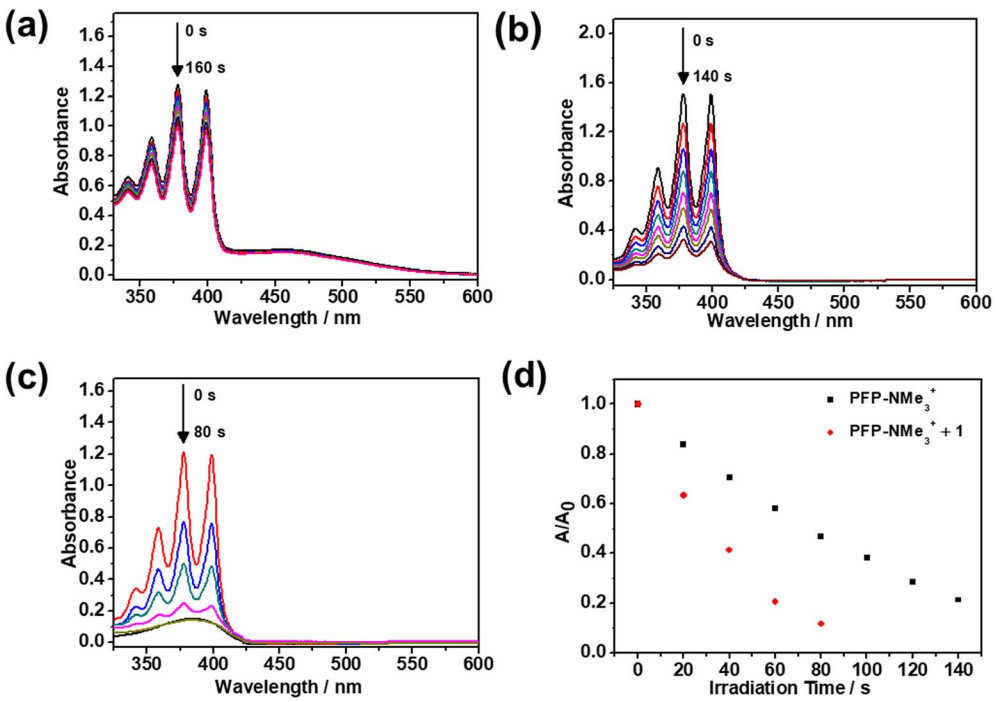

Fig. 6 Electronic absorption spectra of ABDA (100 μM) in the presence of (a) **1**, (b) PFP-NMe_3^+ and (c) ensemble of PFP-NMe_3^+ and **1** in aqueous solution under white light illumination (20 mW cm^{-2}) for different irradiation times. (d) A plot of absorbance changes of ABDA caused by $^1O_2$ oxidation against irradiation time in the presence of PFP-NMe_3^+ and the ensemble of PFP-NMe_3^+ and **1**.

PFP-NMe_3^+. The lack of signals observed in the blue luminescence channel suggests an insignificant disruption of the FRET ensemble by the competitive binding of PFP-NMe_3^+ with the negatively charged pathogen. The existence of the ensemble in confocal images is further supported by incubation of the pathogen with only complex **3**. Particularly, no luminescence signal is observed in the long-wavelength region (Fig. 5i–l), attributed to charge repulsion between the anionic complex **3** and the pathogen. This repulsion deters the assembly of **3** onto the negatively charged surface of the pathogen, further demonstrating the importance of the FRET ensemble, which is stabilized not only by relatively strong electrostatic interactions but also by Pt(II)···Pt(II) and π–π stacking interactions, for the successful imaging of pathogens. It is worth mentioning that the emission of the ensemble facilitated by the FRET process lies in the red optical window which experiences less interference from noise from autofluorescence.[62,63] More importantly, the ^{3}MMLCT emission of **3** is expected to exhibit a longer luminescence lifetime than the fluorescence of PFP-NMe_3^+, and the phosphorescence lifetime of the aggregate form of **3** in the FRET ensemble is found to exhibit an even longer lifetime in the sub-microsecond regime, which could possibly be attributed to a relatively rigid environment experienced by the assembled species (Fig. S10†).[64] This allows further discrimination of background autofluorescence of biological structures by time-gated imaging techniques and makes the ensemble a potential candidate for pathogen imaging in biological environments.

Apart from luminescence imaging, it has been reported that CPEs which include PFP-NMe_3^+ with excellent light-harvesting capabilities are promising candidates for PDT in antibacterial treatment due to their efficient singlet oxygen ($^1O_2$) generation that can induce damage toward pathogens.[65] In view of the strong interactions observed between the negatively charged pathogen and the polymer–metal complex aggregate as reflected from the confocal images, explorations into the performance of the ensemble as a photosensitizer have been made. A commercially available $^1O_2$ sensing probe of 2,2′-(anthracene-9,10-diylbis(methylene))dimalonic acid (ABDA) has been employed to assess the $^1O_2$ generating ability of the two-component system. Under white light illumination (20 mW cm^{-2}), insignificant absorption changes of ABDA in the presence of **1** are observed, suggesting a limited $^1O_2$ generation ability of the complex (Fig. 6a). In sharp contrast, drastic declines in the absorbance are observed in both cases when ABDA is introduced into PFP-NMe_3^+ as well as the ensemble of PFP-NMe_3^+ and **1** (Fig. 6b and c). Compared to PFP-NMe_3^+ alone, the presence of the polyelectrolyte–complex ensemble is found to lead to a more pronounced reduction in the absorption of the ABDA probe, indicating a stronger $^1O_2$ generation ability of the ensemble. A plot showing the spectral degradation of ABDA against irradiation time is obtained to determine the ratio of $^1O_2$ generation quantum yield (Φ_Δ) of PFP-NMe_3^+ and the ensemble (Fig. 6d), in which Φ_Δ corresponding to the ensemble of PFP-NMe_3^+ and **1** is found to be two times higher than that of PFP-NMe_3^+ alone. Such an enhanced $^1O_2$ generation ability of the two-component system highlights the potential of the ensemble as a photosensitizer for PDT.

Conclusion

In conclusion, a series of anionic platinum(II) complexes and their ensembles with PFP-NMe_3^+ have been reported. The anionic complexes are found to assemble with PFP-NMe_3^+ *via* electrostatic, Pt(II)···Pt(II) and π–π stacking interactions to form the polymer–metal complex aggregates. Owing to good spectral overlaps, the complexes have been found to quench the PFP-NMe_3^+ fluorescence through efficient FRET and result in the emergence of ^{3}MMLCT emissions in the low-energy region. The bacteria-binding property of the polyelectrolyte is found to be retained in the two-component ensemble of PFP-NMe_3^+ and **3** compared to PFP-NMe_3^+ alone, which allows the ensemble to serve as an imaging tool for *E. coli* in the red luminescence channel with advantageous features. The low-energy red emission and the extended phosphorescence lifetime of the complex aggregate not only facilitate discrimination of background autofluorescence, but also make time-gated imaging in biological environments possible. The present system is advantageous over the use of cationic CPEs alone or cationic platinum(II) complexes alone for pathogen imaging since the cationic CPEs can emit in the blue channel irrespective of whether they are freely dispersed in solution or are electrostatically assembled on the negatively charged pathogens, leading to a poor imaging contrast between the solution media and the pathogens with a risk of low levels of residual CPE in the culture medium. Similarly, with the cationic platinum(II) complexes alone, the imaging contrast between the freely dispersed orange-emissive platinum(II) complexes in solution and the red-emissive platinum(II) assemblies on the pathogen would be less obvious with a risk of low levels of residual platinum(II) complexes in the culture medium. The current system also has an competitive edge over the use of the anionic CPE–cationic platinum(II) complex counterpart in pathogen imaging, due to its capability to minimize interference from the orange-emissive free anionic platinum(II) complexes or the blue-emissive CPEs and to realize a red luminescence signal by leveraging the efficient FRET process. In addition, the polymer–metal complex ensemble formed from PFP-NMe_3^+ and **1** has shown an enhanced $^1O_2$ generation ability over the polymer alone upon white light illumination, endowing the ensemble with the capability to serve as an attractive photosensitizing agent for PDT. The success in employing ensembles comprising cationic CPEs and anionic platinum(II) complexes in biological applications is anticipated to open new avenues for the development of two-component systems as potential sensing, imaging or therapeutic tools towards cellular components and microorganisms with a negatively charged outer membrane, which cannot be easily achieved by ensembles comprising anionic CPEs and cationic platinum(II) complexes. It is envisaged that this work could also provide insights into strategies for rational design of multi-component platinum(II) systems for various functions and applications.

Data availability

The data supporting this article have been included as part of the ESI.†

Author contributions

V. W.-W. Y. initiated and designed the research. V. W.-W. Y., A. L.-Y. S., J. G. and E. K.-H. W. designed and synthesized the platinum(II) complexes. S. W., H. Y. and Q. S. designed and synthesized the conjugated polyelectrolyte. A. L.-Y. S. and J. G. conducted characterization, photophysical measurements, FRET studies and singlet oxygen generation studies. S. W., H. Y. and Q. S. planned and conducted pathogen imaging experiments. V. W.-W. Y., A. L.-Y. S., J. G. and E. K.-H. W. wrote the manuscript. V. W.-W. Y. and S. W. supervised the work. All authors analyzed the data, discussed the results and contributed to the final manuscript.

Conflicts of interest

There are no conflicts to declare.

Acknowledgements

This work has been supported by the General Research Fund (GRF) (HKU 17311224) and Collaborative Research Fund (CRF) (C7075-21GF) from the Research Grants Council (RGC) of the Hong Kong Special Administrative Region, P. R. China, and the CAS-Croucher Funding Scheme for Joint Laboratories on Molecular Functional Materials for Electronics, Switching, and Sensing. A. L.-Y. S. and J. G. acknowledge the receipt of postgraduate studentships administered by The University of Hong Kong.

References

1 K. Krogmann, Planar Complexes Containing Metal–Metal Bonds, *Angew. Chem., Int. Ed. Engl.*, 1969, **8**, 35–42.
2 K. W. Jennette, S. J. Lippard, G. A. Vassiliades and W. R. Bauer, Metallointercalation Reagents. 2-Hydroxyethanethiolato(2,2',2''-terpyridine)platinum(II) Monocation Binds Strongly to DNA by Intercalation, *Proc. Natl. Acad. Sci. U. S. A.*, 1974, **71**, 3839–3843.
3 R. S. Osborn and D. Rogers, Crystal Structure of the Red Form of 2,2'-Bipyridyldichloroplatinum(II), *J. Chem. Soc., Dalton Trans.*, 1974, 1002–1004.
4 K. W. Jennette, J. T. Gill, J. A. Sadownick and S. J. Lippard, Metallointercalation Reagents. Synthesis, Characterization, and Structural Properties of Thiolato(2,2',2''-terpyridine) platinum(II) Complexes, *J. Am. Chem. Soc.*, 1976, **98**, 6159–6168.
5 V. M. Miskowski and V. H. Houlding, Electronic Spectra and Photophysics of Platinum(II) Complexes with α-Diimine Ligands. Solid-State Effects. 1. Monomers and Ligand π Dimers, *Inorg. Chem.*, 1989, **28**, 1529–1533.
6 V. H. Houlding and V. M. Miskowski, The Effect of Linear Chain Structure on the Electronic Structure of Pt(II) Diimine Complexes, *Coord. Chem. Rev.*, 1991, **111**, 145–152.
7 V. M. Miskowski and V. H. Houlding, Electronic Spectra and Photophysics of Platinum(II) Complexes with α-Diimine Ligands Solid-State Effects. 2. Metal–Metal Interaction in Double Salts and Linear Chains, *Inorg. Chem.*, 1991, **30**, 4446–4452.
8 H.-K. Yip, L.-K. Cheng, K.-K. Cheung and C.-M. Che, Luminescent Platinum(II) Complexes. Electronic Spectroscopy of Platinum(II) Complexes of 2,2':6',2''-Terpyridine (terpy) and *p*-Substituted Phenylterpyridines and Crystal Structure of [Pt(terpy)Cl][CF_3SO_3], *J. Chem. Soc., Dalton Trans.*, 1993, 2933–2938.
9 R. H. Herber, M. Croft, M. J. Coyer, B. Bilash and A. Sahiner, Origin of Polychromism of *Cis* Square-Planar Platinum(II) Complexes: Comparison of Two Forms of [Pt(2,2'-bpy)(Cl_2)], *Inorg. Chem.*, 1994, **33**, 2422–2426.
10 J. A. Bailey, M. G. Hill, R. E. Marsh, V. M. Miskowski, W. P. Schaefer and H. B. Gray, Electronic Spectroscopy of Chloro(terpyridine)platinum(II), *Inorg. Chem.*, 1995, **34**, 4591–4599.
11 W. B. Connick, R. E. Marsh, W. P. Schaefer and H. B. Gray, Linear-Chain Structures of Platinum(II) Diimine Complexes, *Inorg. Chem.*, 1997, **36**, 913–922.
12 G. Arena, G. Calogero, S. Campagna, L. Monsù Scolaro, V. Ricevuto and R. Romeo, Synthesis, Characterization, Absorption Spectra, and Luminescence Properties of Organometallic Platinum(II) Terpyridine Complexes, *Inorg. Chem.*, 1998, **37**, 2763–2769.
13 R. Büchner, C. T. Cunningham, J. S. Field, R. J. Haines, D. R. McMillin and G. C. Summerton, Luminescence Properties of Salts of the $[Pt(4'Ph\text{-}terpy)Cl]^+$ Chromophore: Crystal Structure of the Red Form of [Pt(4'Ph-terpy)Cl]BF_4 (4'Ph-terpy = 4'-Phenyl-2,2':6',2''-terpyridine), *J. Chem. Soc., Dalton Trans.*, 1999, 711–718.
14 V. W.-W. Yam, K. M.-C. Wong and N. Zhu, Solvent-Induced Aggregation through Metal···Metal/π···π Interactions: Large Solvatochromism of Luminescent Organoplatinum(II) Terpyridyl Complexes, *J. Am. Chem. Soc.*, 2002, **124**, 6506–6507.
15 A. J. Goshe, I. M. Steele and B. Bosnich, Supramolecular Recognition. Terpyridyl Palladium and Platinum Molecular Clefts and Their Association with Planar Platinum Complexes, *J. Am. Chem. Soc.*, 2003, **125**, 444–451.
16 V. W.-W. Yam, V. K.-M. Au and S. Y.-L. Leung, Light-Emitting Self-Assembled Materials Based on d^8 and d^{10} Transition Metal Complexes, *Chem. Rev.*, 2015, **115**, 7589–7728.
17 M. H.-Y. Chan and V. W.-W. Yam, Toward the Design and Construction of Supramolecular Functional Molecular Materials Based on Metal–Metal Interactions, *J. Am. Chem. Soc.*, 2022, **144**, 22805–22825.
18 V. W.-W. Yam, Using Synthesis to Steer Excited States and Their Properties and Functions, *Nat. Synth.*, 2023, **2**, 94–100.
19 P. J. Stang, D. H. Cao, S. Saito and A. M. Arif, Self-Assembly of Cationic, Tetranuclear, Pt(II) and Pd(II) Macrocyclic Squares. X-Ray Crystal Structure of $[Pt^{2+}$(dppp)(4,4'-bipyridyl) $2^-OSO_2CF_3]_4$, *J. Am. Chem. Soc.*, 1995, **117**, 6273–6283.
20 R. Romeo, L. M. Scolaro, M. R. Plutino and A. Albinati, Structural Properties of the Metallointercalator Cationic Complex (2,2':6',2''-Terpyridine)methylplatinum(II) Ion, *J. Organomet. Chem.*, 2000, **593–594**, 403–408.

21 K. M.-C. Wong, W.-S. Tang, X.-X. Lu, N. Zhu and V. W.-W. Yam, Functionalized Platinum(II) Terpyridyl Alkynyl Complexes as Colorimetric and Luminescence pH Sensors, *Inorg. Chem.*, 2005, **44**, 1492–1498.

22 C. Po, A. Y.-Y. Tam, K. M.-C. Wong and V. W.-W. Yam, Supramolecular Self-Assembly of Amphiphilic Anionic Platinum(II) Complexes: A Correlation between Spectroscopic and Morphological Properties, *J. Am. Chem. Soc.*, 2011, **133**, 12136–12143.

23 C. Y.-S. Chung and V. W.-W. Yam, Dual pH- and Temperature-Responsive Metallosupramolecular Block Copolymers with Tunable Critical Micelle Temperature by Modulation of the Self-Assembly of NIR-Emissive Alkynylplatinum(II) Complexes Induced by Changes in Hydrophilicity and Electrostatic Effects, *Chem.–Eur. J.*, 2013, **19**, 13182–13192.

24 A. Y.-Y. Tam, K. M.-C. Wong and V. W.-W. Yam, Unusual Luminescence Enhancement of Metallogels of Alkynylplatinum(II) 2,6-Bis(*N*-alkylbenzimidazol-2'-yl) pyridine Complexes upon a Gel-to-Sol Phase Transition at Elevated Temperatures, *J. Am. Chem. Soc.*, 2009, **131**, 6253–6260.

25 V. C.-H. Wong, C. Po, S. Y.-L. Leung, A. K.-W. Chan, S. Yang, B. Zhu, X. Cui and V. W.-W. Yam, Formation of 1D Infinite Chains Directed by Metal–Metal and/or π–π Stacking Interactions of Water-Soluble Platinum(II) 2,6-Bis(benzimidazol-2'-yl)pyridine Double Complex Salts, *J. Am. Chem. Soc.*, 2018, **140**, 657–666.

26 V. W.-W. Yam, K. H.-Y. Chan, K. M.-C. Wong and N. Zhu, Luminescent Platinum(II) Terpyridyl Complexes: Effect of Counter Ions on Solvent-Induced Aggregation and Color Changes, *Chem.–Eur. J.*, 2005, **11**, 4535–4543.

27 C. Yu, K. M.-C. Wong, K. H.-Y. Chan and V. W.-W. Yam, Polymer-Induced Self-Assembly of Alkynylplatinum(II) Terpyridyl Complexes by Metal···Metal/π···π Interactions, *Angew. Chem., Int. Ed.*, 2005, **44**, 791–794.

28 A. S.-Y. Law, L. C.-C. Lee, M. C.-L. Yeung, K. K.-W. Lo and V. W.-W. Yam, Amyloid Protein-Induced Supramolecular Self-Assembly of Water-Soluble Platinum(II) Complexes: A Luminescence Assay for Amyloid Fibrillation Detection and Inhibitor Screening, *J. Am. Chem. Soc.*, 2019, **141**, 18570–18577.

29 Z. Chen, M. H.-Y. Chan and V. W.-W. Yam, Stimuli-Responsive Two-Dimensional Supramolecular Polymers Based on Trinuclear Platinum(II) Scaffolds: Reversible Modulation of Photoluminescence, Cavity Size, and Water Permeability, *J. Am. Chem. Soc.*, 2020, **142**, 16471–16478.

30 K. Zhang and V. W.-W. Yam, Platinum(II) Non-Covalent Crosslinkers for Supramolecular DNA Hydrogels, *Chem. Sci.*, 2020, **11**, 3241–3249.

31 A. S.-Y. Law, L. C.-C. Lee, K. K.-W. Lo and V. W.-W. Yam, Aggregation and Supramolecular Self-Assembly of Low-Energy Red Luminescent Alkynylplatinum(II) Complexes for RNA Detection, Nucleolus Imaging, and RNA Synthesis Inhibitor Screening, *J. Am. Chem. Soc.*, 2021, **143**, 5396–5405.

32 C. W.-T. Chan, A. S.-Y. Law and V. W.-W. Yam, A Luminescence Assay in the Red for the Detection of Hydrogen Peroxide and Glucose Based on Metal Coordination Polyelectrolyte-Induced Supramolecular Self-Assembly of Alkynylplatinum(II) Complexes, *Chem.–Eur. J.*, 2023, **29**, e202300203.

33 C. Y.-S. Chung and V. W.-W. Yam, Induced Self-Assembly and Förster Resonance Energy Transfer Studies of Alkynylplatinum(II) Terpyridine Complex through Interaction with Water-Soluble Poly(phenylene ethynylene sulfonate) and the Proof-of-Principle Demonstration of This Two-Component Ensemble for Selective Label-Free Detection of Human Serum Albumin, *J. Am. Chem. Soc.*, 2011, **133**, 18775–18784.

34 C. Y.-S. Chung and V. W.-W. Yam, Selective Label-Free Detection of G-Quadruplex Structure of Human Telomere by Emission Spectral Changes in Visible-and-NIR Region under Physiological Condition through the FRET of a Two-Component PPE-SO_3^-–Pt(II) Complex Ensemble with Pt···Pt, Electrostatic and π–π Interactions, *Chem. Sci.*, 2013, **4**, 377–387.

35 K. Chan, C. Y.-S. Chung and V. W.-W. Yam, Conjugated Polyelectrolyte-Induced Self-Assembly of Alkynylplatinum(II) 2,6-Bis(benzimidazol-2'-yl)pyridine Complexes, *Chem.–Eur. J.*, 2015, **21**, 16434–16447.

36 K. Chan, C. Y.-S. Chung and V. W.-W. Yam, Parallel Folding Topology-Selective Label-Free Detection and Monitoring of Conformational and Topological Changes of Different G-Quadruplex DNAs by Emission Spectral Changes *via* FRET of *m*PPE-Ala–Pt(II) Complex Ensemble, *Chem. Sci.*, 2016, **7**, 2842–2855.

37 B. G. De Geest, R. E. Vandenbroucke, A. M. Guenther, G. B. Sukhorukov, W. E. Hennink, N. N. Sanders, J. Demeester and S. C. De Smedt, Intracellularly Degradable Polyelectrolyte Microcapsules, *Adv. Mater.*, 2006, **18**, 1005–1009.

38 S. Wu, M. Zhu, D. Lu, A. H. Milani, Q. Lian, L. A. Fielding, B. R. Saunders, M. J. Derry, S. P. Armes, D. Adlam and J. A. Hoyland, Self-Curing Super-Stretchable Polymer/Microgel Complex Coacervate Gels without Covalent Bond Formation, *Chem. Sci.*, 2019, **10**, 8832–8839.

39 W. He, M. Wang, G. Mei, S. Liu, A. Q. Khan, C. Li, D. Feng, Z. Su, L. Bao, G. Wang, E. Liu, Y. Zhu, J. Bai, M. Zhu, X. Zhou and Z. Liu, Establishing Superfine Nanofibrils for Robust Polyelectrolyte Artificial Spider Silk and Powerful Artificial Muscles, *Nat. Commun.*, 2024, **15**, 3485.

40 L. Mazzaferro, T. M. Grasseschi, B. D. Like, M. J. Panzer and A. Asatekin, Amphiphilic Polyelectrolyte Complexes for Fouling-Resistant and Easily Tunable Membranes, *ACS Appl. Mater. Interfaces*, 2024, **16**, 37952–37962.

41 Q. Zhou and T. M. Swager, Fluorescent Chemosensors Based on Energy Migration in Conjugated Polymers: The Molecular Wire Approach to Increased Sensitivity, *J. Am. Chem. Soc.*, 1995, **117**, 12593–12602.

42 T. M. Swager, The Molecular Wire Approach to Sensory Signal Amplification, *Acc. Chem. Res.*, 1998, **31**, 201–207.

43 H. Jiang, X. Zhao and K. S. Schanze, Amplified Fluorescence Quenching of a Conjugated Polyelectrolyte Mediated by Ca^{2+}, *Langmuir*, 2006, **22**, 5541–5543.

44 C. W.-T. Chan, K. Chan and V. W.-W. Yam, Induced Self-Assembly and Disassembly of Alkynylplatinum(II) 2,6-Bis(benzimidazol-2'-yl)pyridine Complexes with Charge Reversal Properties: "Proof-of-Principle" Demonstration of Ratiometric Förster Resonance Energy Transfer Sensing of pH, *ACS Appl. Mater. Interfaces*, 2023, **15**, 25122–25133.

45 S. W. Botchway, M. Charnley, J. W. Haycock, A. W. Parker, D. L. Rochester, J. A. Weinstein and J. A. G. Williams, Time-Resolved and Two-Photon Emission Imaging Microscopy of Live Cells with Inert Platinum Complexes, *Proc. Natl. Acad. Sci. U. S. A.*, 2008, **105**, 16071–16076.

46 C. Y.-S. Chung, S. P.-Y. Li, M.-W. Louie, K. K.-W. Lo and V. W.-W. Yam, Induced Self-Assembly and Disassembly of Water-Soluble Alkynylplatinum(II) Terpyridyl Complexes with "Switchable" Near-Infrared (NIR) Emission Modulated by Metal–Metal Interactions over Physiological pH: Demonstration of pH-Responsive NIR Luminescent Probes in Cell-Imaging Studies, *Chem. Sci.*, 2013, **4**, 2453–2462.

47 M. Mauro, A. Aliprandi, D. Septiadi, N. S. Kehr and L. De Cola, When Self-Assembly Meets Biology: Luminescent Platinum Complexes for Imaging Applications, *Chem. Soc. Rev.*, 2014, **43**, 4144–4166.

48 K. Li, G. S.-M. Tong, Q. Wan, G. Cheng, W.-Y. Tong, W.-H. Ang, W.-L. Kwong and C.-M. Che, Highly Phosphorescent Platinum(II) Emitters: Photophysics, Materials and Biological Applications, *Chem. Sci.*, 2016, **7**, 1653–1673.

49 K. Zhang, M. C.-L. Yeung, S. Y.-L. Leung and V. W.-W. Yam, Platinum(II) Probes for Sensing Polyelectrolyte Lengths and Architectures, *ACS Appl. Mater. Interfaces*, 2020, **12**, 8503–8512.

50 B. S. Gaylord, A. J. Heeger and G. C. Bazan, DNA Detection Using Water-Soluble Conjugated Polymers and Peptide Nucleic Acid Probes, *Proc. Natl. Acad. Sci. U. S. A.*, 2002, **99**, 10954–10957.

51 S. Wang, B. S. Gaylord and G. C. Bazan, Fluorescein Provides a Resonance Gate for FRET from Conjugated Polymers to DNA Intercalated Dyes, *J. Am. Chem. Soc.*, 2004, **126**, 5446–5451.

52 F. He, Y. Tang, M. Yu, S. Wang, Y. Li and D. Zhu, Fluorescence-Amplifying Detection of Hydrogen Peroxide with Cationic Conjugated Polymers, and Its Application to Glucose Sensing, *Adv. Funct. Mater.*, 2006, **16**, 91–94.

53 B. Liu and G. C. Bazan, Energy Transfer Between a Cationic-Conjugated Poly(fluorene-*co*-phenylene) and Thiazole Orange for DNA Hybridization Detection Involving G-Rich Sequences, *Macromol. Rapid Commun.*, 2007, **28**, 1804–1808.

54 H. Bai, H. Chen, R. Hu, M. Li, F. Lv, L. Liu and S. Wang, Supramolecular Conjugated Polymer Materials for *in Situ* Pathogen Detection, *ACS Appl. Mater. Interfaces*, 2016, **8**, 31550–31557.

55 Y. Zeng, X. Zhou, R. Qi, N. Dai, X. Fu, H. Zhao, K. Peng, H. Yuan, Y. Huang, F. Lv, L. Liu and S. Wang, Photoactive Conjugated Polymer-Based Hybrid Biosystems for Enhancing Cyanobacterial Photosynthesis and Regulating Redox State of Protein, *Adv. Funct. Mater.*, 2021, **31**, 2007814.

56 R. Qi, F. Lv, Y. Zeng, Q. Shen, Y. Huang, H. Bai, L. Liu and S. Wang, Photoactive Conjugated Polymer-Based Strategy to Effectively Inactivate RNA Viruses, *NPG Asia Mater.*, 2023, **15**, 17.

57 Y.-S. Wong, F. C.-M. Leung, M. Ng, H.-K. Cheng and V. W.-W. Yam, Platinum(II)-Based Supramolecular Scaffold-Templated Side-by-Side Assembly of Gold Nanorods through Pt···Pt and π–π Interactions, *Angew. Chem., Int. Ed.*, 2018, **57**, 15797–15801.

58 Y. Liu, K. Ogawa and K. S. Schanze, Conjugated Polyelectrolytes as Fluorescent Sensors, *J. Photochem. Photobiol., C*, 2009, **10**, 173–190.

59 J. P. Guthrie, Hydrolysis of Esters of Oxy Acids: pK_a Values for Strong Acids; Brønsted Relationship for Attack of Water at Methyl; Free Energies of Hydrolysis of Esters of Oxy Acids; and a Linear Relationship Between Free Energy of Hydrolysis and pK_a Holding over a Range of 20 pK Units, *Can. J. Chem.*, 1978, **56**, 2342–2354.

60 H. Yuan, Z. Liu, L. Liu, F. Lv, Y. Wang and S. Wang, Cationic Conjugated Polymers for Discrimination of Microbial Pathogens, *Adv. Mater.*, 2014, **26**, 4333–4338.

61 H. Yuan, H. Zhao, K. Peng, R. Qi, H. Bai, P. Zhang, Y. Huang, F. Lv, L. Liu, J. Bao and S. Wang, Conjugated Polymer-Quantum Dot Hybrid Materials for Pathogen Discrimination and Disinfection, *ACS Appl. Mater. Interfaces*, 2020, **12**, 21263–21269.

62 J. V. Frangioni, *In Vivo* Near-Infrared Fluorescence Imaging, *Curr. Opin. Chem. Biol.*, 2003, **7**, 626–634.

63 E. A. Owens, M. Henary, G. El Fakhri and H. S. Choi, Tissue-Specific Near-Infrared Fluorescence Imaging, *Acc. Chem. Res.*, 2016, **49**, 1731–1740.

64 A. A. Martí, Metal Complexes and Time-Resolved Photoluminescence Spectroscopy for Sensing Applications, *J. Photochem. Photobiol., A*, 2015, **307–308**, 35–47.

65 W. Wu, G. C. Bazan and B. Liu, Conjugated-Polymer-Amplified Sensing, Imaging, and Therapy, *Chem*, 2017, **2**, 760–790.